# Strong neutron-transfer coupling effects in the reaction mechanism of the $^{18}O + ^{64}Zn$ system at energies near the Coulomb barrier

E. Crema,[1,*] B. Paes,[2] V. A. B. Zagatto,[1,2] J. F. P. Huiza,[3] J. Lubian,[2] J. M. B. Shorto,[4] R. F. Simões,[1] D. S. Monteiro,[5,6] N. Added,[1] M. C. Morais,[7] and P. R. S. Gomes[2,1,†]

[1]*Departamento de Física Nuclear, Instituto de Física da Universidade de São Paulo, Caixa Postal 66318, São Paulo, São Paulo 05315-970, Brazil*

[2]*Instituto de Física, Universidade Federal Fluminense, Avenida Litorânea s/n, Gragoatá, Niterói, Rio de Janeiro 24210-340, Brazil*

[3]*Universidade Estadual do Sudoeste da Bahia, Bahia, Brazil*

[4]*Instituto de Pesquisas Energéticas e Nucleares, IPEN/CNEN, São Paulo, São Paulo 05508-000, Brazil*

[5]*ILACVN, Universidade Federal da Integração Latino-Americana, Foz do Iguaçu, Paraná 85866-000, Brazil*

[6]*Department of Physics, University of Notre Dame, South Bend, Indiana 46556, USA*

[7]*INFES, Universidade Federal Fluminense, Santo Antonio de Pádua, Rio de Janeiro 28470 000, Brazil*

(Received 26 July 2019; revised manuscript received 10 October 2019; published 14 November 2019)

The precise quasielastic excitation function for the $^{18}O + ^{64}Zn$ system was measured at energies near and below the Coulomb barrier at $\theta_{lab} = 161^{\circ}$, from which its correlated quasielastic barrier distribution was derived. The excitation functions for the two-neutron, $\alpha$, and tritium transfer reactions have also been measured at the same conditions. These data were well described by the coupled channel and coupled reaction channel calculations. The comparison of the data with theoretical calculations shows the strong influence of three inelastic channels in the coupling process: the quadrupole and octupole vibrational states of $^{64}Zn$, $2_1^+$ and $3_1^-$, and the quadrupole vibrational state of $^{18}O$, $2_1^+$. In addition, theoretical calculations indicate that the two-neutron stripping is mostly due to a one-step process, which has a striking effect on the reaction mechanism of this system.

DOI: 10.1103/PhysRevC.100.054608

## I. INTRODUCTION

Direct reactions between nuclei are essential processes in the synthesis of elements within stars, since they can be the doorway to nuclear fusion at low collision energies. These reactions can also act as intermediate steps in the complex fusion process between heavy nuclei during the synthesis of superheavy elements. Particularly relevant to these two situations are neutron transfers, since the absence of electric repulsion facilitates the passage of neutrons from one nucleus to another. On the other hand, from experimental and theoretical points of view, direct reactions between nuclei have been crucial instruments in the investigation of both nuclear structure and reaction mechanisms [1,2]. As these processes are strongly dependent on nuclear structures of the interacting nuclei, it is difficult to extrapolate results from one system to others. So, it is important to carry out systematic studies to understand the dependence of each reaction channel as a function of structural details of colliding nuclei in different mass regions.

As more detailed and fundamental calculations are available, it has become possible to investigate the role of the pairing interaction during transfer processes. For example, recent studies on two-neutron transfer reactions with the projectile $^{18}O$ have shown that, while a one-step process dominates when $^{12}C$, $^{13}C$, and $^{16}O$ targets are involved [3–6], in the case of heavier targets such as $^{28}Si$ and $^{64}Ni$ the sequential transfer of two neutrons should also be invoked to explain some experimental data [7,8]. Usually, the works in the literature dedicated to this subject, including those mentioned above, only analyze the angular dependence of the direct reactions investigated. However, for a complete understanding of the reaction mechanism of a system, it is also necessary to study the dependence of its reaction channels on the bombarding energy, and how each channel is coupled to other ones. In recent decades, it has been demonstrated that barrier distribution methods (fusion and quasielastic) are powerful tools for investigating the energy dependence and couplings of nuclear and Coulomb processes that occur in collisions between nuclei at energies around the Coulomb barrier. An interesting feature of quasielastic barrier distributions (QEBDs) is that they are obtained with simpler experiments than fusion barrier distributions. In addition, as quasielastic and fusion are complementary processes, both barrier distributions carry approximately the same information about the reaction mechanism at energies around the Coulomb barrier [9–13]. In particular, QEBDs have been successfully used in describing reaction channel couplings in systems involving both light and heavy nuclei [9–21]. The sensitivity of QEBDs has even allowed the precise evaluation of the nuclear matter diffusivity of nuclei

*crema@if.usp.br

†Deceased.

 

such as $^{17}$O, $^{18}$O, and $^{48}$Ca [16,18,19]. The comparison of large coupled reaction channel (CRC) calculations with the experimental QEBD of the $^{48}$Ca + $^{120}$Sn system has indicated that the pairing correlation has significant importance in its reaction dynamics, indicating that barrier distribution methods can be also used to investigate this phenomenon [19].

The present work is the conclusion of a comparative study of the energy dependence of several direct processes that occur in the $^{16,17,18}$O + $^{64}$Zn systems at energies around the Coulomb barrier. For this purpose, a precise quasielastic excitation function was measured for the $^{18}$O + $^{64}$Zn system at backward angles, from which its barrier distribution could be deduced. Excitation functions (EFs) for two-neutron, tritium, and $\alpha$ transfers, at the same energies and angle, were also measured.

The projectile $^{18}$O was chosen because its neutron pair outside the $^{16}$O core is relatively easily transferred from projectile to target even in collisions at energies around the Coulomb barrier, and the pairing correlation can be tested. Besides, the $^{16}$O core is very stable and, in principle, it does not participate actively in the reaction mechanism at low bombarding energies (the same has also been observed at higher energies [3–6,16,18,19,22]). On the other hand, the $^{64}$Zn target was chosen because there is room in its outer $1f_{5/2}$ neutron subshell to accept the two neutrons from the projectile. The choice of this system will allow an interesting comparison with the neighbor $^{18}$O + $^{63}$Cu system that we have already studied, since the two targets have the same configuration of neutrons [21].

The other two systems of this systematic study, $^{16,17}$O + $^{64}$Zn, have been studied previously [16,17], whereby it was demonstrated that the barrier distribution method is sensitive enough to investigate the relative importance of the reaction channels in the collision dynamics of these systems.

At energies around the Coulomb barrier, where deep inelastic collisions are less probable, quasielastic scattering is defined as the sum of elastic scattering, inelastic scattering, and all reaction processes with an exchange of a small number of nucleons between the interacting nuclei. It is well known that the QEBD is obtained from the first derivative of the ratio of the quasielastic cross section ($\sigma_{\rm qel}$) to the Rutherford cross section ($\sigma_{\rm Ruth}$) with respect to energy: $d(-d\sigma_{\rm qel}/d\sigma_{\rm Ruth})/dE$ [10].

The theoretical approach of this paper is based on extensive coupled channel (CC) and coupled reaction channel calculations in which the real interaction between projectile and target is described by the double-folding São Paulo potential (SPP) [23]. As described elsewhere, the crucial aspect of our theoretical approach is that no imaginary potential at the interaction barrier region is employed in the entrance channel [9,16–21]. The fusion process is accounted for by an inner (related to the nominal Coulomb barrier) imaginary Woods-Saxon potential, in such a way that variations of 10% in its parameters do not affect the results significantly. Our calculations can also be considered as being parameter free in the sense that the SPP employs the two-parameter-Fermi shape for which the radius and diffuseness parameters are calculated, averaging hundreds of experimental and theoretical values. Then, all the available reaction channels are introduced into the coupling matrix, one by one, to investigate their individual effects on the reaction dynamics. Therefore, our purpose is not to fit data by varying potential parameters but only to compare data with the theoretical results.

This paper is organized as follows. In Sec. II, the experimental results are presented and discussed. The details of our theoretical calculations and the comparison of their results to data are given in Sec. III. Finally, the main conclusions are presented in Sec. IV.

## II. THE EXPERIMENT

The $^{18}$O beams employed in this experiment were delivered by the 8UD electrostatic accelerator of the Pelletron laboratory of the University of São Paulo. The beams, in the energy range of $E_{\rm lab}$ = 30–45 MeV (in steps of 1 MeV and intensities from 10–70 p nA), bombarded a self-supporting target of 40 $\mu$g/cm$^2$ of $^{64}$Zn isotope enriched to 99.9%. The nuclei coming from the reactions were detected and identified by means of $\Delta E$-$E$ spectra, where the $\Delta E$ signals were the energy losses in the gas of a proportional counter placed at $\theta_{\rm LAB} = 161^\circ$, which contained a silicon barrier detector in its back to measure the residual energy, $E$. Three surface barrier detectors were placed at forward angles ($\pm 30^\circ$ and $45^\circ$) for normalization purposes. For most energies the statistical uncertainties were below 1% and for the highest ones they were around 3%. The background was properly subtracted. The essential point of barrier distribution methods is the derivative of experimental data with respect to the beam energy. So, to get reasonable results it is crucial that the measurement of bombarding energies, as well as the energy steps, be very precise and coherent. That is why electrostatic accelerators with a beam analyzing magnet are ideal tools for this kind of investigation. However, the differential hysteresis effects must be minimized by recycling the magnet as described by Leigh *et al.* [24]. In the present paper, we followed the same procedure described in that work with the method of recycling the magnet by Spear *et al.* [25]. Our absolute beam energies were defined to about 60 keV, and the coherence of data was checked by repeating several measurements in the excitation function.

Figure 1 shows $\Delta E$-$E$ spectra for the $^{16,17,18}$O + $^{64}$Zn systems [panels (a)–(c), respectively], where we can qualitatively compare the most probable transfer reactions that occur in them. As can be seen, the $Z$ resolution is good enough to identify the different reaction products. It is possible to distinguish elastic and inelastic scatterings ($Z$ = 8), transfers of few nucleons ($Z$ = 6, 7, 8, 9, and 10), and stripping of two neutrons. It should be emphasized that this experiment was designed for the inclusive measurement of the quasielastic scattering. The spectra shown in Fig. 1 were taken at approximately the same energies, and they have roughly the same numbers of events in the quasielastic peak, which allows a qualitative comparison of their reaction mechanisms. The major difference between them is the absence in the $^{16}$O + $^{64}$Zn system of events with energy above the elastic group, while in the $^{17,18}$O + $^{64}$Zn systems we observe events in that region corresponding to the one-neutron and two-neutron transfer

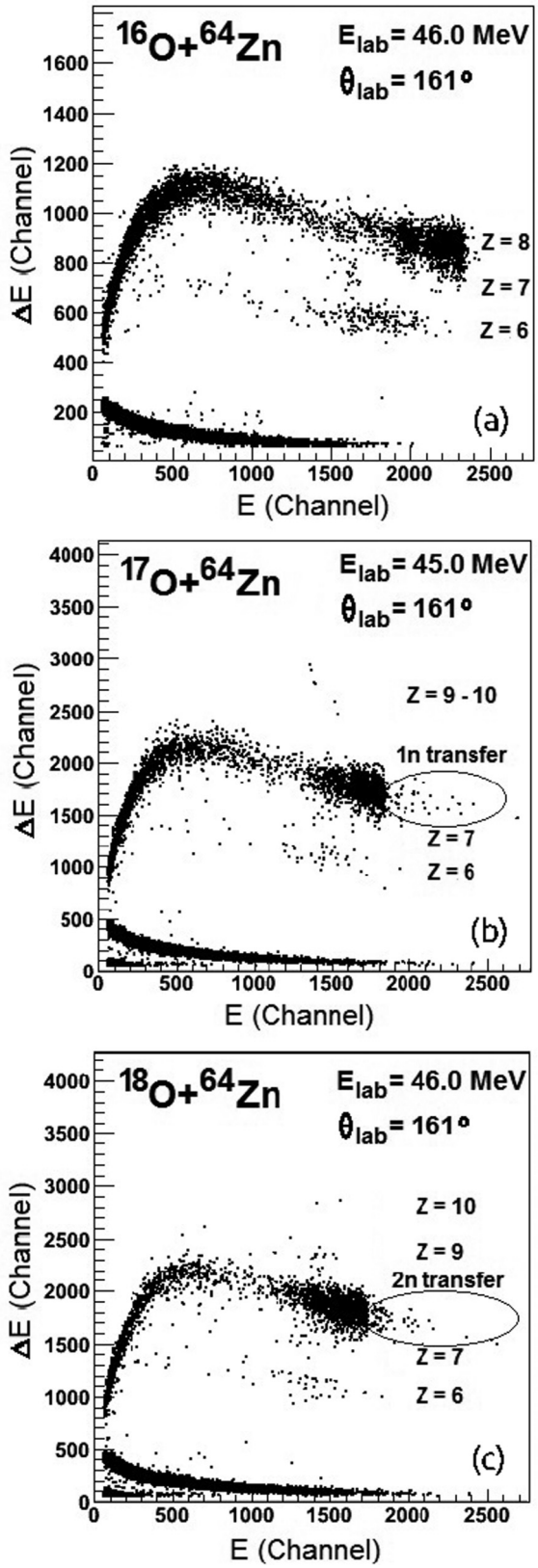


FIG. 1. $\Delta E$-$E$ spectra for the $^{16,17,18}\mathrm{O} + {}^{64}\mathrm{Zn}$ systems taken at the same angle and approximately the same energies. These spectra have approximately the same number of events in the elastic peak to allow a direct and qualitative comparison of their reaction mechanisms.

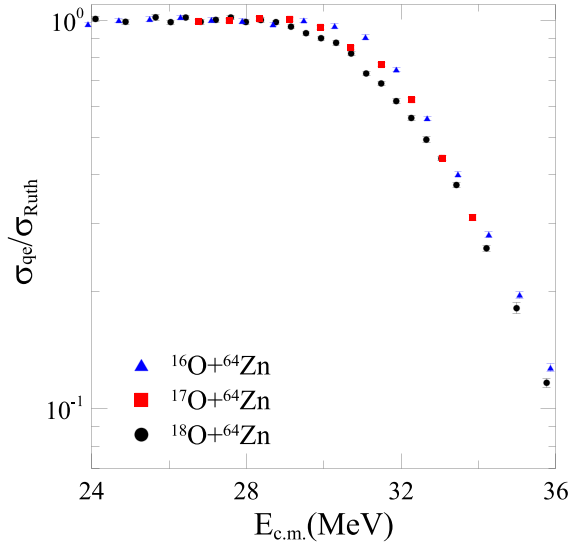


FIG. 2. Quasielastic excitation functions for the $^{16,17,18}\mathrm{O} + {}^{64}\mathrm{Zn}$ systems taken at $\theta_{\mathrm{lab}} = 161^{\circ}$. See the text for details.

reactions that have positive $Q_{\mathrm{gg}}$ values equal to $+3.8$ and $+6.8$ MeV, respectively. On the other hand, the events with $Z = 6$, which mostly correspond to the $\alpha$-particle stripping, seem to be more favored in the case of the $^{16}$O projectile, indicating that the presence of neutrons outside the $^{16}$O core hinders this process. It is interesting to observe that some pickup events with $\Delta Z = 1$ and 2 are observed for the $^{17,18}$O projectiles, while none of these events occur with the $^{16}$O projectile. Also, the pickup events with $\Delta Z = 1$ are more probable when $^{18}$O is used as a projectile. As will be shown in the following, these events correspond mainly to tritium stripping processes.

From the spectrum analysis, a precise quasielastic EF for the $^{18}\mathrm{O} + {}^{64}\mathrm{Zn}$ system was measured. Figure 2 shows the comparison between the EFs for the $^{16,17,18}\mathrm{O} + {}^{64}\mathrm{Zn}$ systems. As can be seen, at energies below 28 MeV and above 33 MeV, the three EFs have similar behavior. However, between these energies, the EFs for the $^{17,18}\mathrm{O} + {}^{64}\mathrm{Zn}$ systems decrease faster than that for the $^{16}\mathrm{O} + {}^{64}\mathrm{Zn}$ system. But it is the structure of the $^{18}$O projectile that produces a more remarkable effect. It is interesting to note that the difference between these three systems is more accentuated below their Coulomb barriers (32 MeV, approximately).

From the quasielastic EF for the $^{18}\mathrm{O} + {}^{64}\mathrm{Zn}$ presented before, its corresponding QEBD was deduced, which is shown in Fig. 3 compared to the ones for the $^{16,17}\mathrm{O} + {}^{64}\mathrm{Zn}$ systems. All these QEBDs were deduced by using the point difference method with the same energy step (2 MeV in the laboratory framework) [10,11]. All theoretical calculations that will be presented later in this paper were calculated in the same way. In this figure, where the $^{16}\mathrm{O} + {}^{64}\mathrm{Zn}$ system was taken as reference, the influence in the reaction mechanisms of the number of neutrons outside the $^{16}$O core becomes more evident. As is well known [26], in the reactions between heavy ions, several reaction channels are opened, which, by quantum interference, can be coupled with each other. In the framework of the barrier distribution models, this reaction

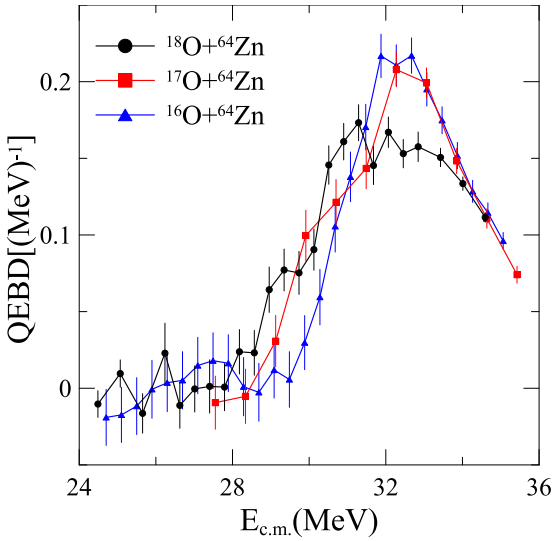


FIG. 3. quasielastic barrier distribution for the $^{16,17,18}$O + $^{64}$Zn systems. See the text for details.

channel interference replaces the single Coulomb barrier with a barrier distribution. Coupling of reaction channels with positive $Q_{gg}$ values produces new barriers in the distribution at energies below the main Coulomb barrier, while the coupling of channels with negative $Q_{gg}$ values has their barriers placed at energies above the Coulomb barrier. The stronger the coupling, the more intense the effect on the distribution will be. Therefore, the simple and qualitative analysis of a barrier distribution allows one to discover not only the presence of strongly coupled channels but also some details of these channels. From this point of view, Fig. 3 shows that new barriers were added to the QEBDs of the $^{17,18}$O + $^{64}$Zn systems at energies below the Coulomb barrier, indicating that some channels with positive $Q_{gg}$ values are strongly coupled in these systems. It should be noted that the couplings produced by the two extra neutrons of the $^{18}$O projectile are very intense and produce a large flattening of the QEBD because, as the total area of the distribution is unitary, the appearance of new reaction barriers must be compensated with the decrease of the main peak. As will be demonstrated by the calculations of the next sections, the main reaction channels responsible for the effects observed in Fig. 3 are the one- and two-neutron transfers.

Several measurements of QEBDs have already been performed and a lot of data are available in the literature. Certainly, a comparison of the present data with those previously obtained becomes necessary. However, one should be cautious when making such comparison because the present system is lighter than others previously reported. Barrier distributions may be multipeaked, which is usually associated with the strong coupling of highly collective excited states of nuclei involved. An example may be seen in Fig. 2 of Ref. [27] for $^{20}$Ne + $^{90}$Zr. The same fingerprint of strong coupling was verified in the $^{20}$Ne +$^{58,60}$ Ni systems, as one may observe in Fig. 4 of Ref. [28]. It is also well known that such multipeaked behavior may be annulled by the coupling of noncollective single-particle states to the coupling scheme, as demonstrated in the $^{20}$Ne + $^{92}$Zr [27] and $^{20}$Ne + $^{61}$Ni [28] systems. One may observe that the density of energy levels in $^{92}$Zr and $^{61}$Ni nuclei is much higher than those present in the previously mentioned isotopes. The same occurs with $^{63,65}$Cu isotopes [20,21,29,30] as well as with the present $^{64}$Zn nucleus, explaining why only one peak is observed in these QEBDs.

On the other hand, barrier distributions measured for heavier systems have shown the importance of projectile excitation to the coupling scheme ($^{28}$Si + $^{154}$Sm of Ref. [31]) or became important for studying superheavy elements ($^{54}$Cr + $^{208}$Pb of Ref. [32]). The present work may contribute to the study of some of the same effects in a lower mass region which is less investigated in the literature and is more accessible to laboratories with limited bombarding energies.

As stated by Ref. [33], fusion barrier distributions and QEBDs are both important (and complementary) to completely understand all the processes which a given nuclear reaction may undergo. This way, the comprehension of the QEBD and processes that define its shape may result in valuable information when confronted with nuclear fusion data for the same system [10]. Several structures observed in low energy data of fusion barrier distributions are usually associated with transfer reactions with positive $Q$ values. The $^{32}$S + $^{110}$Pd fusion barrier distribution shows an extra structure when compared to $^{36}$S + $^{110}$Pd system, due to the high $Q$ value of the two-neutron pickup process of the former [34]. A similar effect has been reported for the $^{40,48}$Ca + $^{96}$Zr systems [11,35,36], where the fusion excitation function for the $^{40}$Ca projectile is well described only when neutron transfer channels are coupled to the elastic channel. Such transfer channels are suppressed in the $^{48}$Ca case. One may conclude that, given the already proven importance of transfer processes and their influence on fusion barrier distributions, studying the same effects in QEBDs becomes highly desirable.

## III. THEORETICAL ANALYSIS

In this section, we study the dynamics of the $^{18}$O + $^{64}$Zn reaction by including a different kind of coupling to the elastic channels, step by step. First, we study the effect of collective excitations of the projectile and target on the quasielastic EF and QEBD by performing coupled channel calculations. After that, we include different transfer channels, for which the excitation function could be extracted from the experimental spectrum, by performing CRC calculations. The rearrangement channels included were the one-neutron, two-neutron, tritium, and $\alpha$ transfers.

In all our calculations, the FRESCO code [37] was used. For the real part of the optical potential, the double folding SPP was used. This potential is a double-folding potential calculated with the two-parameter Fermi shape for both the nuclear and charge densities. Experimental and theoretical values of these charge and matter parameters available in the literature for a large number of nuclei have been analyzed and show systematic behaviors with little dispersion around average values. In this sense, a SPP constructed with these average parameters can be considered a parameter-free interaction. Some exceptions depart from the systematic

values of 0.56 fm obtained for the diffuseness of the two-parameter Fermi-Dirac matter density distribution. This is, for example, the case of the $^{18,17}$O isotopes. For $^{18}$O there was obtained a value of 0.60 fm [18] while for $^{17}$O a value of 0.62 fm [17] was found from the study of the QEBDs for the $^{18}$O + $^{58}$Ni and $^{17}$O + $^{64}$Zn reactions, respectively. The imaginary part included in our calculations was meant only to account for the loss of flux going to the projectile-target fusion. Any effect from direct reaction channels will be included explicitly in the coupling scheme. So, no imaginary surface potential will be added in any of our calculations to account for any direct-reaction channel effect. To warrant this property of the imaginary part of the nuclear potential, we used a Woods-Saxon potential with parameters $W = 80$ MeV, $r_w = 0.9$, fm and $a_w = 0.2$ fm for the depth, reduced radius, and diffuseness, respectively. This methodology was recently used to study the quasielastic excitation functions (EFs) and QEBDs of the $^{18,16}$O + $^{63,65}$Cu [20,21,29,30]. We would like to emphasize, nevertheless, that any change of the parameters of this Woods-Saxon absorptive potential does not change the results of calculations, as long as it remains located at distances shorter than the position of the top of the Coulomb barrier [17,18,20,21,29,30].

The SPP was also used for both the real and imaginary parts of the nuclear potential in the final partitions in all finite-range CRC calculations. The strength coefficients $(1.0 + 0.78i)V_{SPP}$ were used. This procedure was also used in all the transfer reactions previously cited above [3–6,16–18,18–22,29,30]. These systematic studies correspond to the situation when no couplings are considered among the states in the final partition. It has been proved that this is a reasonable approximation for describing the elastic scattering when no strong couplings to these channels are expected [38]. In the coupling matrix elements, a complex remnant was adopted, and prior representation of the interacting potentials was used.

To generate single-particle or cluster wave functions a Woods-Saxon potential was used with a reduced radius equal to 1.27 fm and diffuseness of 0.7 fm. The depths of the potential were varied to fit the corresponding experimental value for the separation of that particle (cluster). In the case of the one-neutron and tritium transfer reactions, a spin-orbit interaction was included, using the same geometrical parameters, and a depth of 7 MeV was fixed.

### A. Inelastic couplings

To study the effect of the projectile and target inelastic channels on the quasielastic EF and QEBD we performed CC calculations, including the first excited state of the projectile, the $2^+$ at 1.98 MeV, and some excited states of the target, shown on Table I. In this table, the reduced transition probabilities used to couple different target states are also shown. As the experimental values are used for the reduced transition probabilities, one can say that our calculations are model independent or a variant of the second-order anharmonic vibrational model [39]. The transition potentials were taken, as usual, as the derivative of the Coulomb and real part of the nuclear potential.

TABLE I. States included in the coupling scheme of the CC calculation and electric reduced transition probabilities used to derive the coupling matrix element between states. $\pi$ and n mean the parity and order of appearance of the spin $I$. $\langle M \rangle$ are derived from the $B(E\lambda)$.

| Nucleus | $I^\pi_{n,i}$ | $I^\pi_{n,f}$ | $I_f$ Energy (MeV) | $\langle M \rangle$ | Ref. |
|---|---|---|---|---|---|
| $^{18}$O | $0^+_1$(g.s.) | $2^+_1$ | 1.98 | 6.71 | [40] |
| | $0^+_1$(g.s.) | $2^+_1$ | 0.99 | 40.00 | [40] |
| | $0^+_1$(g.s.) | $2^+_2$ | 1.79 | 1.91 | [41] |
| $^{64}$Zn | $2^+_1$ | $0^+_2$ | 1.91 | 0.93 | [41] |
| | $2^+_1$ | $4^+_1$ | 2.30 | 40.86 | [41] |
| | $0^+_1$(g.s.) | $3^-_1$ | 2.99 | 184.39 | [42] |

In Fig. 4 the results of our CC calculations are compared with the experimental data for the quasielastic EF [panel (a)] and the corresponding QEBD [panel (b)]. The thin red line represents a calculation when only the ground states of the projectile and target were considered. By comparing to the experimental data, one realizes the need for couplings of different reaction mechanisms to obtain a better agreement with the data. The dashed green line represents the effect of the coupling to the first excited state of the target (including its reorientation). The impact of the coupling of this state to the

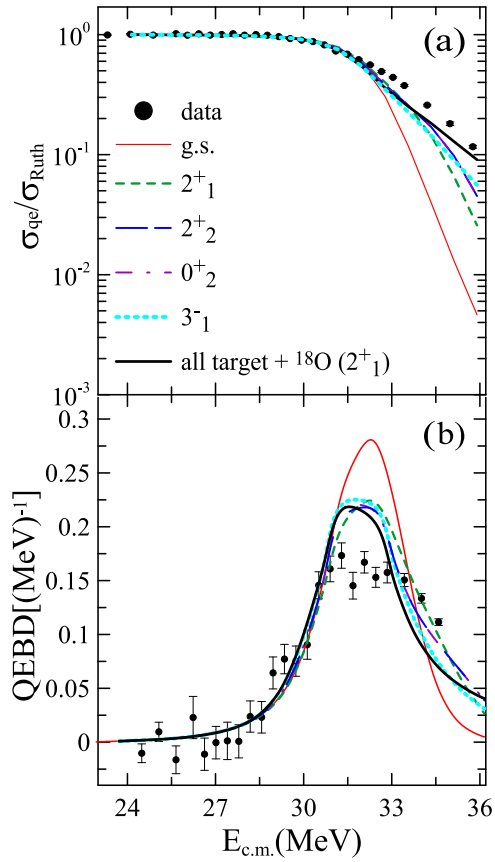


FIG. 4. Effect of target and projectile inelastic couplings on the quasielastic EF (a) and QEBD (b) for the $^{18}$O + $^{64}$Zn reaction. See the text for details.

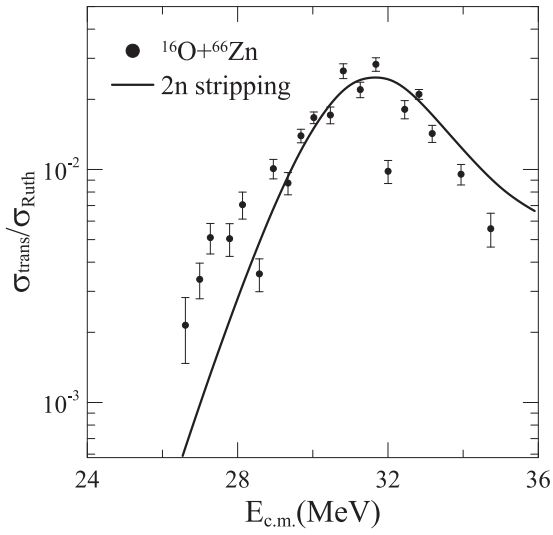


FIG. 5. Excitation function of the $^{64}$Zn($^{18}$O, $^{16}$O)$^{66}$Zn two-neutron transfer reaction at near barrier energies.

TABLE II. List of states of the residual $^{66}$Zn nucleus for which two-neutron transfer cross section was calculated.

| $I^{\pi}$ | Energy (MeV) |
|---|---|
| $0^+$ | 0.0 |
| $3^-$ | 4.4720 |
| $4^+$ | 4.5380 |
| $3^-$ | 4.5650 |
| $5^-$ | 4.5670 |
| $4^+$ | 4.6100 |
| $4^+$ | 4.6940 |
| $2^+$ | 4.7300 |
| $5^-$ | 4.7800 |
| $7^-$ | 4.8140 |
| $8^+$ | 5.2073 |
| $9^-$ | 5.4644 |
| $3^-$ | 5.6500 |
| $10^+$ | 6.2926 |
| $8^+$ | 6.8500 |

elastic channel is quite relevant, due to the strong collectivity of the target. The other collective states of the target have a minor relevance to the quasielastic EF and QEBD. The ones that have some cumulative effect (adding one by one to the previous coupling scheme) were the $2_2^+$ (long-dash–short-dashed blue line), the $0_2^+$ (short-dash–dotted magenta line), and the first octupole state (dotted cyan line). The first excited stated of the projectile also has some relevance in the reaction mechanism. The effect of the coupling of this state can be deduced from the thick black line in Fig. 4, which represents the sum of all couplings. It should be noted that the contribution of this projectile excitation is very relevant at higher energies. The other states included in the coupling scheme that do not affect the quasielastic EF and QEBD are not shown in the figure.

The uncoupled barrier distribution represented by the red line in Fig. 4(b) is associated with the single Coulomb barrier generated by the bare potential. From the same figure, one can see that the total effect of the inelastic couplings [black line in Fig. 4(b)] was to shift the entire QEBD towards lower energies. So, this result indicates that the excitation of the inelastic channels can lead to an increase of the fusion cross section in the investigated system, as expected [26,43].

Having exhausted the study of the effect of the collective degrees of freedom, in the next subsections we study the most relevant transfer channels observed in the experimental spectrum.

### B. Two-neutron transfer

We have measured the excitation function for the two-neutron transfer process in the $^{18}$O + $^{64}$Zn system, and the experimental results are presented in Fig. 5. We start the theoretical study of the rearrangement reactions on the reaction mechanism by studying the effect of the two-neutron transfer channel on the quasielastic EF and QEBD. It was recently observed that for similar systems $^{18}$O + $^{63,65}$Cu [21,30] the two-neutron transfer channel was the one that most affected the EF and the QEBD, although the most relevant ones were the excitation of collective states of the projectile and target, as in the present study. This is quite understandable, since the low-lying state wave functions of the $^{18}$O nucleus have been proved to have a strong two-neutron component, and can be considered in many reactions as an inert core of $^{16}$O plus two neutrons bound to it [4–8]. In the $^{18}$O + $^{64}$Zn system, the $Q$ value of the two-neutron transfer reaction is very positive ($Q_{g.s.} = 6.849$ MeV). For this reason, it is expected that highly excited states of the residual nuclei should also contribute to the EF. At his high excitation energy, the state density of the residual $^{66}$Zn is quite high, and the experimental spectroscopy for states in this energy region is scarce. Many of the states in this region do not have a correct spin-parity assignment (being doubtful or even nonexistent). Considering this, we included the particle transfer to a group of states of $^{66}$Zn ranging from 4.5 up to 7 MeV of excitation energy for which there exists more reliable spectroscopic information. The list of $^{66}$Zn states for which the two-neutron cross section was calculated is given in Table II.

Due to the high density states of the residual nucleus $^{66}$Zn and the absence of experimental spectroscopic information for most of these states, we did not perform microscopic calculations to determine spectroscopic amplitudes for the two neutron overlaps. Instead, we used the cluster model in which the internal structure of the two neutrons is neglected, and they are considered to be in the 1$s$ wave configuration, i.e., antiparallel with total spin 0. In this case, the two-neutron transfer becomes similar to the transfer of a single particle with a mass of two units, and with quantum numbers determined by their relative angular momentum to the core, $L$, and the main quantum number $N$. These quantum numbers are determined from the conservation of the total quantum number carrier by each neutron, according to the single-particle orbital it is occupying.

For the spectroscopic amplitudes of the projectile and ejectile and of the target and residual nucleus, the global value

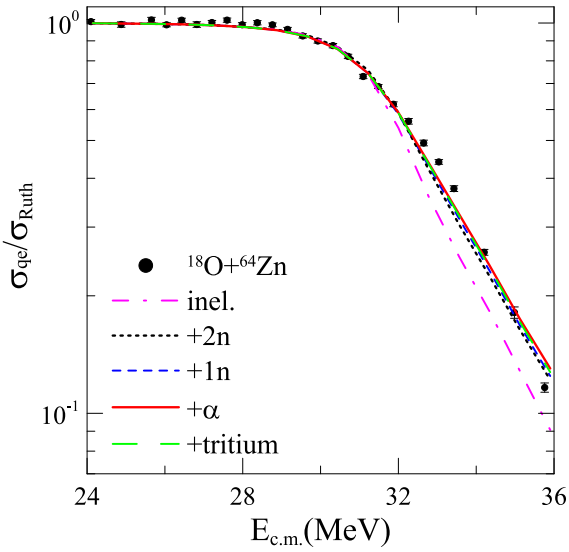


FIG. 6. Effect of rearrangement channels on the quasielastic EF. The contributions of the various transfer channels are added cumulatively, one by one, from the result of the inelastic channel obtained in the previous section. See the text for details.

of 0.95 was assumed. These values guaranteed a quite reasonable agreement with the experimental excitation function for the two-neutron transfer processes, as shown in Fig. 5. Although this calculation is approximate, the agreement with the experimental data allows us to estimate the contribution of the two-neutron channel to the quasielastic EF and QEBD. This is shown in Fig. 6 for the EF and Fig. 7 for the QEBD by the black dotted lines. It is important to mention that what is represented by 2*n* in the legends of these figures is the result of CRC calculation, including, besides the two-neutron

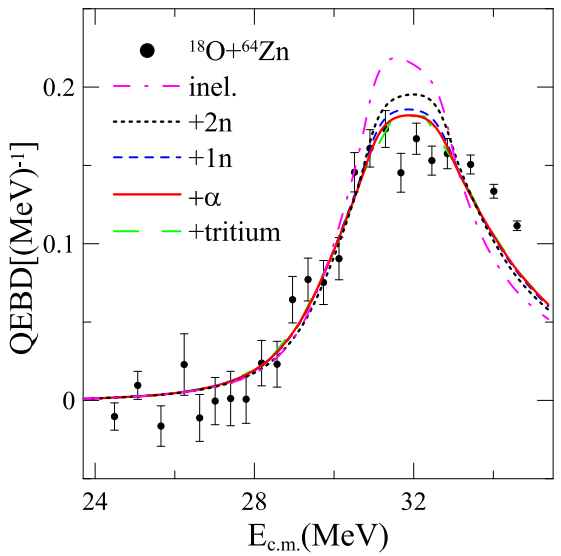


FIG. 7. Effect of rearrangement channels on the QEBD. The contributions of the various transfer channels are added cumulatively, one by one, from the result of the inelastic channel obtained in the previous section. See the text for details.

transfer channels, all the inelastic channels discussed in the previous subsection. In these figures, the cumulative effect of the inclusion of other rearrangement channels is also shown. The details will be given in the next subsections. One observes from Figs. 6 and 7 that the two-neutron transfer channel has a strong influence on the EF and QEBD. Similar results, as anticipated at the beginning of this subsection, were recently obtained for the $^{18}$O + $^{63,65}$Cu reactions [21,30]. Another important conclusion that can be derived from Fig. 7 is that this channel increases the effective barrier, as can be seen by the small shift toward higher energies of the main peak of the barrier distribution. The reason for that is that, although the target and the residual nucleus have the same deformation, the projectile is more deformed than the ejectile, which is a spherical double-magic nucleus. As demonstrated in Refs. [44–46], the transfer reactions enhanceS the fusion cross section if, as a result of the rearrangement, the residual nuclei are more deformed than the initial nuclei, the net effect of which is to decrease the Coulomb barrier. As in our case the residual nuclei are less deformed, an increment of the Coulomb barrier is expected.

The effect of the low-lying states of $^{66}$Zn on the two-neutron EF was verified, and a very small contribution was observed. Other channels, like excitation of the projectile and/or target followed by a two-neutron transfer, might influence the two-neutron excitation function [5,8] and consequently the global value of the spectroscopic amplitude that fits it. However, as the present data are inclusive, it is not possible to perform such a microscopic study of the individual mechanisms of reaction for each channel. Nevertheless, the amount of flux that goes to this two-neutron channel was correctly described, as it is dictated by the experimental EF.

### C. One-neutron transfer

The ground state *Q* value of the reaction $^{64}$Zn($^{18}$O, $^{17}$O)$^{65}$Zn is equal to −0.066 MeV, indicating that the probability of this reaction mechanism should not be very high at energies around the Coulomb barrier. At low energies, only the low energy states of the residual nuclei should contribute to the cross section of this reaction. When the incident energy of the projectile increases, more channels could be opened. Nevertheless, their contribution to the barrier region should be small, although there might be some contribution at the higher energies. The $^{17}$O ejectile is in the same *Z* line of the elastically scattered $^{18}$O. Therefore, the reaction products are under the quasielastic peak, and it is not possible to directly measure this reaction cross section in our experiment. On the other hand, as the states that should have the larger cross section are the lower ones of the $^{65}$Zn, it is possible to perform shell-model calculations to determine the spectroscopic amplitudes of the projectile and target overlaps. For this purpose, we performed calculations using the NUSHELLX code [47] to derive the spectroscopic amplitudes of the $\langle^{64}\text{Zn}|^{65}\text{Zn}\rangle$ overlaps. In the shell-model calculations, the model space *bjuff* [8] and the effective phenomenological interaction of Ref. [48] were derived from the CD-Bonn *NN* potential renormalized by the so-called $V_{\text{low-}k}$ approach [49,50]. This interaction was developed for

TABLE III. Spectroscopic amplitudes used in the CRC calculations for one-neutron transfer reactions, where $j$ is the spin of the neutron orbitals.

| Initial state | $j$ | Final state | Spect. ampl. |
|---|---|---|---|
| $^{18}O_{g.s.}(0^+)$ | $(1d_{5/2})$ | $^{17}O_{g.s}(5/2^+)$ | 1.305 |
| $^{18}O_{g.s.}(0^+)$ | $(2s_{1/2})$ | $^{17}O_{0.807}(1/2^+)$ | −0.561 |
| $^{18}O_{g.s.}(0^+)$ | $(1p_{1/2})$ | $^{17}O_{3.055}(1/2^-)$ | −0.929 |
| $^{18}O_{1.982}(2^+)$ | $(1d_{5/2})$ | $^{17}O_{g.s}(5/2^+)$ | 0.929 |
| | $(2s_{1/2})$ | | 0.666 |
| $^{18}O_{1.982}(2^+)$ | $(1d_{5/2})$ | $^{17}O_{0.807}(1/2^+)$ | −0.652 |
| $^{64}Zn_{g.s.}(0^+)$ | $(1f_{5/2})$ | $^{65}Zn_{g.s.}(5/2^-)$ | 0.690 |
| $^{64}Zn_{g.s.}(0^+)$ | $(2p_{3/2})$ | $^{65}Zn_{0.115}(3/2^-)$ | −0.198 |
| $^{64}Zn_{g.s.}(0^+)$ | $(2p_{3/2})$ | $^{65}Zn_{0.207}(3/2^-)$ | 0.419 |
| $^{64}Zn_{g.s.}(0^+)$ | $(1f_{5/2})$ | $^{65}Zn_{0.768}(5/2^-)$ | 0.059 |
| $^{64}Zn_{g.s.}(0^+)$ | $(2p_{1/2})$ | $^{65}Zn_{0.866}(1/2^-)$ | 0.458 |
| | $(1f_{5/2})$ | | −0.411 |
| $^{64}Zn_{0.991}(2^+)$ | $(2p_{3/2})$ | $^{65}Zn_{g.s.}(5/2^-)$ | −0.101 |
| | $(2p_{1/2})$ | | 0.059 |
| | $(1f_{5/2})$ | | 0.770 |
| $^{64}Zn_{0.991}(2^+)$ | $(2p_{3/2})$ | $^{65}Zn_{0.115}(3/2^+)$ | 0.412 |
| | $(2p_{1/2})$ | | −0.396 |
| | $(1f_{5/2})$ | | 0.611 |
| $^{64}Zn_{0.991}(2^+)$ | $(2p_{3/2})$ | $^{65}Zn_{0.207}(3/2^-)$ | −0.235 |
| | $(2p_{1/2})$ | | 0.247 |
| | $(1f_{5/2})$ | | 0.396 |
| $^{64}Zn_{0.991}(2^+)$ | $(2p_{3/2})$ | $^{65}Zn_{0.768}(5/2^-)$ | −0.134 |
| | $(2p_{1/2})$ | | −0.365 |
| $^{64}Zn_{0.991}(2^+)$ | $(1f_{5/2})$ | $^{65}Zn_{0.864}(7/2^-)$ | 0.040 |
| | $(2p_{3/2})$ | | −0.266 |
| $^{64}Zn_{0.991}(2^+)$ | $(1f_{5/2})$ | $^{65}Zn_{0.866}(1/2^-)$ | 0.347 |
| | $(2p_{3/2})$ | | −0.750 |

nickel isotopes with mass and charge near the ones of $^{64}$Zn. So, it is expected that it will be possible to reproduce the structure characteristics of the $^{64,65}$Zn isotopes as well. This model space allow us to describe the experimental energy spectra of the $^{64,65}$Zn isotopes with good agreement with differences lower than 300 keV up to the excitation energies of 0.991 MeV ($2^+$) for the $^{64}$Zn nucleus and 0.115 MeV ($3/2^-$), 0.768 MeV ($5/2^-$), and 0.864 MeV ($7/2^-$) for the $^{65}$Zn nucleus. In this model space, the valence particles can populate the $1f_{7/2}$ and $2p_{3/2}$ orbitals for protons and the $2p_{3/2}$, $1f_{5/2}$, $2p_{1/2}$, and $1g_{9/2}$ orbitals for neutrons. The spectroscopic amplitudes for the target overlaps needed for the one-neutron transfer cross section calculations, using the $^{48}$Ca as core, are listed in Table III. The spectroscopic amplitudes for the $\langle^{18}\text{O}|^{17}\text{O}\rangle$ overlaps were taken from Ref. [8].

In Figs. 6 and 7 the result of the CRC calculation including the collective, two-neutron-, and one-neutron transfer channels for the quasielastic EF and QEBD are shown by blue dashed lines. One realizes from these calculations that the effect of the one-neutron transfer channel on the reaction mechanism is very small. The same result was recently observed in the case of $^{18}\text{O} + ^{63,65}$Cu reactions [21,30]. This might be an indication of the relevance of the pairing correlation in the two-neutron transfer reaction, as this reaction mechanism was the most important in all the mentioned reactions. Moreover,

TABLE IV. List of states of the residual $^{67}$Ga nucleus for which tritium transfer cross section was calculated.

| $I^\pi$ | Energy (MeV) |
|---|---|
| $3/2^-$ | 0.0 |
| $1/2^-$ | 0.167 |
| $5/2^-$ | 0.359 |
| $3/2^-$ | 0.828 |
| $5/2^-$ | 0.911 |
| $1/2^-$ | 1.082 |
| $7/2^-$ | 1.202 |
| $7/2^-$ | 1.412 |
| $5/2^-$ | 1.554 |
| $3/2^-$ | 1.639 |
| $3/2^-$ | 1.809 |
| $5/2^-$ | 2.04 |
| $3/2^-$ | 2.141 |
| $3/2^-$ | 2.172 |
| $7/2^-$ | 2.176 |
| $7/2^-$ | 2.281 |
| $7/2^-$ | 2.651 |
| $3/2^-$ | 2.73 |
| $3/2^-$ | 2.942 |
| $3/2^-$ | 3.036 |
| $3/2^-$ | 3.225 |

the one-neutron transfer is the first step in the sequential two-neutron transfer mechanism, and it was found to be a very weak channel.

### D. Other rearrangement reactions: Tritium and α transfer reactions

Among the charged-particle rearrangement reactions that might affect the quasielastic EF and QEBD are the transfer of a proton, deuteron, tritium, or $\alpha$ particle. The spectra in Fig. 1 shows that in our measurements we detected events with $Z = 7$, which could correspond to the proton, deuteron, or tritium stripping processes. As the proton and deuteron stripping have very negative $Q$ values ($Q = -11.999$ and $-8.747$ MeV, respectively), the events with Z = 7 were considered as mainly produced by the tritium stripping that has a nearly zero $Q$ value ($Q = -0.09$ MeV). In Fig. 1, we can see stripping events with $Z = 6$, which were considered as having been produced by $\alpha$ stripping reactions ($Q = -2.564$ MeV). So, the experimental excitation functions for these stripping processes were measured and are shown in Figs. 8 and 9. Nevertheless, as these are massive particles and the $Q$ values are negative, the cross sections of these reactions are expected to be small.

We performed, first, CRC calculations, including the coupling to the tritium channel. As in the case of the two-neutron transfer reaction, the cluster model was used, and only transfers from the ground state of the projectile and target were considered. The reason is the same as before. We are interested in determining the correct amount of reaction flux that goes to this channel by fitting the experimental data

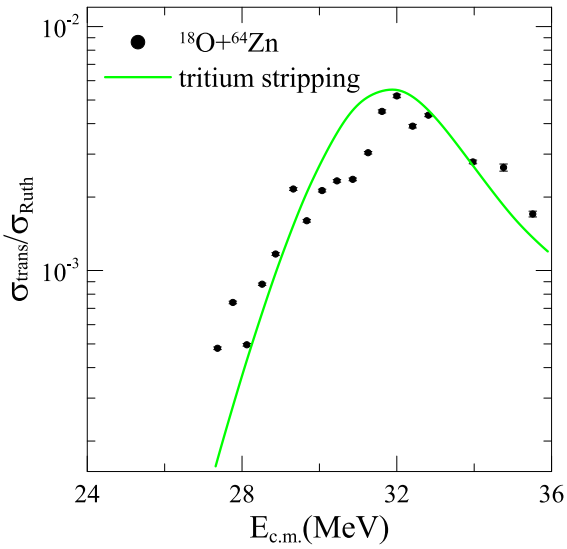


FIG. 8. Excitation function of the $^{64}$Zn($^{18}$O, $^{15}$N)$^{67}$Ga tritium transfer reaction at near barrier energies.

(that are inclusive). The list of the states of $^{67}$Ga that were summed in the EF of the tritium transfer reaction is shown in Table IV. The $^{17}$N was assumed to remain in its ground state. The overall spectroscopic amplitude for all the target overlaps that yielded a good agreement of the theoretical calculation with the experimental data was 0.3. In Fig. 8 the results of our calculations are compared with the experimental data of the tritium EF.

In Figs. 6 and 7 the results of the CRC calculation including the collective, two-neutron, one-neutron and tritium transfer channels for the quasielastic EF and QEBD are shown by green long-dashed lines. From these figures, one observes that the effect of the tritium transfer channel on the quasielastic EF and QEBD is very small.

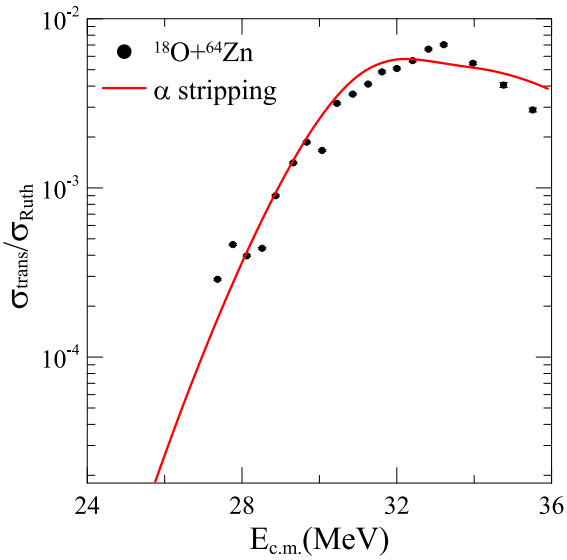


FIG. 9. Excitation function of the $^{64}$Zn($^{18}$O, $^{14}$N)$^{68}$Ga $\alpha$ transfer reaction at near barrier energies.

TABLE V. List of states of the residual $^{68}$Ga nucleus for which the $\alpha$ transfer cross section was calculated.

| $I^{\pi}$ | Energy (MeV) |
|---|---|
| $0^+$ | 0.0 |
| $2^+$ | 1.015 |
| $0^+$ | 1.754 |
| $2^+$ | 1.777 |
| $4^+$ | 2.267 |
| $2^+$ | 2.457 |
| $3^+$ | 2.648 |
| $4^+$ | 2.831 |
| $2^+$ | 2.947 |
| $2^+$ | 3.023 |
| $4^+$ | 3.182 |
| $0^+$ | 3.204 |
| $2^+$ | 3.4 |

To finish our study of the reaction mechanism for the $^{18}$O + $^{64}$Zn at energies near the Coulomb barrier, we included in our previous CRC calculation the $\alpha$ transfer channel. Again, the cluster model was used, which in this case is the more natural model to be used. Only transfers from the ground state of the projectile were included, and the ejectile was considered to be formed only in the ground state. The list of the states of $^{68}$Ga that were incorporated in the theoretical $\alpha$ EF using a global spectroscopic amplitude of 0.28 is shown in Table V. The comparison of the theoretical and experimental EFs for the $\alpha$ transfer channel is shown in Fig. 9. A very good agreement with the experimental data is observed.

A comparison of the results of the full CRC cross section (full red line) with the experimental data of the quasielastic EF and QEBD is shown in Figs. 6 and 7, respectively. One can see that the agreement of the theoretical results and the experimental data is good. Also, one clearly sees that the effect of the $\alpha$ transfer channel is very small. This result is in agreement with the results for the of $^{18}$O + $^{63,65}$Cu reactions [21,30], for which the effect of the transfer of charged massive particles on the EF and QEBD was also found to be very small.

## IV. CONCLUSIONS

In the context of a large systematic study that we are undertaking, we reported new experimental data for the system $^{18}$O + $^{64}$Zn at energies around the Coulomb barrier. The experimental quasielastic barrier distribution for this system was deduced from a high precision quasielastic excitation function measured at the backward angle of $\theta_{lab} = 161^{\circ}$. Excitation functions for the two-neutron, tritium, and $\alpha$-stripping processes were also measured at the same angle and energies. We compared the new data obtained in this work with the neighbor systems $^{17}$O + $^{64}$Zn and $^{18}$O + $^{64}$Zn, which we measured previously. The simple qualitative comparison of the $\Delta E$-$E$ spectra with similar statistics of these three systems allowed us to observe the main differences of their reaction mechanisms. The major difference between them is the absence in the $^{16}$O + $^{64}$Zn system of events with energy

above the elastic group, while in the $^{17,18}O + {}^{64}Zn$ systems we observe events in that region corresponding to the one-neutron and two-neutrons transfer reactions that have positive $Q_{gg}$ values, equal to +3.8 and +6.8 MeV, respectively. On the other hand, the events with $Z = 6$, which mostly correspond to $\alpha$ particle stripping, seem to be more favored in the case of the $^{16}O$ projectile, indicating that the presence of neutrons outside the $^{16}O$ core hinders this process. It is worth noting that few pickup events with $\Delta Z = 1$ and 2 are observed for the $^{17,18}O$ projectiles, while none of these events occurs with the $^{16}O$ projectile.

The qualitative comparison between the quasielastic excitation functions and the quasielastic barrier distributions for the three systems has permitted us to conclude that the extra neutrons in the $^{17}O$ and $^{18}O$ isotopes, compared to the $^{16}O$ one, have a strong influence on the reaction dynamics of these systems. This effect is much more important in the $^{18}O + {}^{64}Zn$ system, which presents a very flat quasielastic barrier distribution that is characteristic of systems with strong coupled channels. It is also interesting to observe that neighbor systems that we have measured, such as $^{18}O + {}^{63,65}Cu$, have less flattened distributions.

The experimental quasielastic EF and the corresponding QEBD were compared with CRC calculations that included collective excitations of the projectile and target (including the reorientation of the first excited states of both nuclei) and the one-neutron, two-neutron, tritium, and $\alpha$ transfer channels. A quite good description of both quasielastic EF and QEBD was obtained, allowing us to state that the main ingredients of the reaction mechanism were considered in the CRC calculations. It was observed that the channels that produce a stronger effect on the quasielastic EF and QEBD were the collective excitations of the $^{18}O$ and $^{64}Zn$ nuclei plus the two-neutron transfer channel. As the one-neutron transfer channel was found to be of minor relevance for the reaction mechanism, we suggest that the two-neutron transfer might be dominated by direct (one-step) transfer enhanced by the pairing correlation between the two transferred neutrons.

## ACKNOWLEDGMENTS

This work was financially supported by FAPESP, CNPq, CAPES, FAPERJ, and INCT-FNA (Instituto Nacional de Ciência e Tecnologia- Física Nuclear e Aplicações) (Proc. No. 464898/2014-5). One of the authors, E.C., thanks CNPq (Proc. No. 305228/2015-3) for financial support. We would like to thank the technical staff of Pelletron Laboratory for assisting in the maintenance and operation of the accelerator.

[1] G. R. Satchler, *Direct Nuclear Reactions* (Oxford University Press, Oxford, 1983).
[2] R. A. Broglia and A. Winther, *Heavy Ion Reactions* (Westview, Boulder, CO, 2004).
[3] M. Cavallaro, F. Cappuzzello, M. Bondì, D. Carbone, V. N. Garcia, A. Gargano, S. M. Lenzi, J. Lubian, C. Agodi, F. Azaiez, M. De Napoli, A. Foti, S. Franchoo, R. Linares, D. Nicolosi, M. Niikura, J. A. Scarpaci, and S. Tropea, Phys. Rev. C **88**, 054601 (2013).
[4] D. Carbone, J. L. Ferreira, F. Cappuzzello, J. Lubian, C. Agodi, M. Cavallaro, A. Foti, A. Gargano, S. M. Lenzi, R. Linares, and G. Santagati, Phys. Rev. C **95**, 034603 (2017).
[5] M. J. Ermamatov, F. Cappuzzello, J. Lubian, M. Cubero, C. Agodi, D. Carbone, M. Cavallaro, J. L. Ferreira, A. Foti, V. N. Garcia, A. Gargano, J. A. Lay, S. M. Lenzi, R. Linares, G. Santagati, and A. Vitturi, Phys. Rev. C **94**, 024610 (2016).
[6] M. J. Ermamatov, R. Linares, J. Lubian, J. L. Ferreira, F. Cappuzzello, D. Carbone, M. Cavallaro, M. Cubero, P. N. de Faria, A. Foti, G. Santagati, and V. A. B. Zagatto, Phys. Rev. C **96**, 044603 (2017).
[7] E. N. Cardozo, J. Lubian, R. Linares, F. Cappuzzello, D. Carbone, M. Cavallaro, J. L. Ferreira, A. Gargano, B. Paes, and G. Santagati, Phys. Rev. C **97**, 064611 (2018).
[8] B. Paes, G. Santagati, R. M. Vsevolodovna, F. Cappuzzello, D. Carbone, E. N. Cardozo, M. Cavallaro, H. Garcia-Tecocoatzi, A. Gargano, J. L. Ferreira, S. M. Lenzi, R. Linares, E. Santopinto, A. Vitturi, and J. Lubian, Phys. Rev. C **96**, 044612 (2017).
[9] R. F. Simões, D. S. Monteiro, L. K. Ono, A. M. Jacob, J. M. B. Shorto, N. Added, and E. Crema, Phys Lett. B **527**, 187 (2002).
[10] H. Timmers, J. R. Leigh, M. Dasgupta, D. J. Hinde, R. C. Lemmon, J. C. Mein, C. R. Morton, J. O. Newton, and N. Rowley, Nucl. Phys. A **584**, 190 (1995).
[11] H. Timmers, D. Ackermann, S. Beghini, L. Corradi, J. H. He, G. Montagnoli, F. Scarlassara, A. M. Stefanini, and N. Rowley, Nucl. Phys. A **633**, 421 (1998).
[12] M. Dasgupta, D. J. Hinde, N. Rowley, and A. M. Stefanini, Annu. Rev. Nucl. Part. Sci. **48**, 401 (1998).
[13] N. Rowley, H. Timmers, J. R. Leigh, M. Dasgupta, D. J. Hinde, J. C. Mein, C. R. Morton, and J. O. Newton, Phys. Lett. B **373**, 23 (1996).
[14] N. Rowley, G. R. Satchler, and P. H. Stelson, Phys. Lett. B **254**, 25 (1991).
[15] A. T. Kruppa, E. Romain, M. A. Nagarajan, and N. Rowley, Nucl. Phys. A **560**, 845 (1993).
[16] J. F. P. Huiza, E. Crema, D. S. Monteiro, J. M. B. Shorto, R. F. Simões, N. Added, and P. R. S. Gomes, Phys. Rev. C **75**, 064601 (2007).
[17] J. F. P. Huiza, E. Crema, A. Barioni, D. S. Monteiro, J. M. B. Shorto, R. F. Simões, and P. R. S. Gomes, Phys. Rev. C **82**, 054603 (2010).
[18] E. Crema, D. R. Otomar, R. F. Simões, A. Barioni, D. S. Monteiro, L. K. Ono, J. M. B. Shorto, J. Lubian, and P. R. S. Gomes, Phys. Rev. C **84**, 024601 (2011).
[19] E. Crema, M. A. G. Alvarez, N. H. Medina, L. R. Gasques, J. F. P. Huiza, B. Fernández, Z. Abou-Haidar, P. N. de Faria, P. R. S. Gomes, J. Lubian, and D. Verney, Phys. Rev. C **88**, 044616 (2013).
[20] J. M. B. Shorto, E. Crema, R. F. Simões, D. S. Monteiro, J. F. P. Huiza, N. Added, and P. R. S. Gomes, Phys. Rev. C **78**, 064610 (2008).

[21] E. Crema, V. A. B. Zagatto, J. M. B. Shorto, B. Paes, J. Lubian, R. F. Simões, D. S. Monteiro, J. F. P. Huiza, N. Added, M. C. Morais, and P. R. S. Gomes, Phys. Rev. C **98**, 044614 (2018).
[22] F. Cappuzzello, D. Carbone, M. Cavallaro, M. Bondì, C. Agodi, F. Azaiez, A. Bonaccorso, A. Cunsolo, L. Fortunato, A. Foti *et al.*, Nat. Commun. **6**, 6743 (2015).
[23] L. C. Chamon, B. V. Carlson, L. R. Gasques, D. Pereira *et al.*, Phys. Rev. C **66**, 014610 (2002).
[24] J. R. Leigh, M. Dasgupta, D. J. Hinde, J. C. Mein, C. R. Morton, R. C. Lemmon, J. P. Lestone, J. O. Newton, H. Timmers, and J. X. Wei, Phys. Rev. C **52**, 3151 (1995)
[25] R. H. Spear, D. C. Kean, M. T. Esat, A. N. R. Joye, and M. P. Fewell, Nucl. Instrum. Methods **147**, 455 (1977).
[26] L. F. Canto, P. R. S. Gomes, R. Donangelo, and M. S. Hussein, Phys. Rep. **424**, 1 (2006).
[27] E. Piasecki, L. Swiderski, W. Gawlikowicz, J. Jastrzebski, N. Keeley, M. Kisielinski, S. Kliczewski *et al.*, Phys. Rev. C **80**, 054613 (2009).
[28] A. Trzcińska, E. Piasecki, K. Hagino, W. Czarnacki, P. Decowski, N. Keeley, M. Kisieliński, P. Koczoń, A. Kordyasz, E. Koshchiy, M. Kowalczyk, B. Lommel, A. Stolarz, I. Strojek, and K. Zerva, Phys. Rev. C **92**, 034619 (2015).
[29] E. Crema, V. A. B. Zagatto, J. M. B. Shorto, B. Paes, J. Lubian, R. F. Simoes, D. S. Monteiro, J. F. P. Huiza, N. Added, M. C. Morais, and P. R. S. Gomes, Phys. Rev. C **99**, 054623 (2019).
[30] V. A. B. Zagatto, E. Crema, J. M. B. Shorto, M. C. Morais, J. Lubian, N. Added, R. F. Simões, D. S. Monteiro, J. F. P. Huiza, B. Paes, and P. R. S. Gomes, Phys. Rev. C **100**, 044602 (2019).
[31] G. Kaur, B. R. Behera, A. Jhingan, B. K. Nayak, R. Dubey, P. Sharma, M. Thakur, R. Mahajan, N. Saneesh, T. Banerjee, Khushboo, A. Kumar, S. Mandal, A. Saxena, P. Sugathan, and N. Rowley, Phys. Rev. C **94**, 034613 (2016).
[32] S. Mitsuoka, H. Ikezoe, K. Nishio, K. Tsuruta, S. C. Jeong, and Y. Watanabe, Phys. Rev. Lett. **99**, 182701 (2007).
[33] G. Montagnoli and A. M. Stefanini, Eur. Phys. J. A **53**, 169 (2017).
[34] A. M. Stefanini, D. Ackermann, L. Corradi, J. H. He, G. Montagnoli, S. Beghini, F. Scarlassara, and G. F. Segato, Phys. Rev. C **52**, R1727 (1995).
[35] H. Timmers, L. Corradi, A. M. Stefanini, D. Ackermann, J. H. He, S. Beghini, G. Montagnoli, F. Scarlassara, G. F. Segato, and N. Rowley, Phys. Lett. B **399**, 35 (1997).
[36] A. M. Stefanini, G. Montagnoli, H. Esbensen, L. Corradi, S. Courtin, E. Fioretto, A. Goasduff, J. Grebosz, F. Haas, M. Mazzocco, C. Michelagnoli, T. Mijatović, D. Montanari, G. Pasqualato, C. Parascandolo, F. Scarlassara, E. Strano, S. Szilner, and D. Torresi, Phys. Lett. B **728**, 639 (2014).
[37] I. J. Thompson, http://www.fresco.org.uk
[38] L. R. Gasques, L. C. Chamon, P. R. S. Gomes, and J. Lubian, Nucl. Phys. A **764**, 135 (2006).
[39] J. Lubian and R. Cabezas, J. Phys. G, Nucl. and Part. Phys. **19**, 1201 (1993).
[40] S. Raman, C. W. Nestor, Jr., and P. Tikkanen, At. Data Nucl. Data Tables **78**, 1 (2001).
[41] https://www.nndc.bnl.gov/ensdf/
[42] T. Kibédi and R. H. Spear, At. Data Nucl. Data Tables **80**, 35 (2002).
[43] L. F. Canto, P. R. S. Gomes, R. Donangelo, J. Lubian, and M. S. Hussein, Phys. Rep. **596**, 1 (2015).
[44] V. V. Sargsyan, G. G. Adamian, N. V. Antonenko, W. Scheid, and H. Q. Zhang, Phys. Rev. C **84**, 064614 (2011).
[45] V. V. Sargsyan, G. G. Adamian, N. V. Antonenko, W. Scheid, and H. Q. Zhang, Phys. Rev. C **85**, 024616 (2012).
[46] V. V. Sargsyan, G. G. Adamian, N. V. Antonenko, W. Scheid, and H. Q. Zhang, Phys. Rev. C **86**, 014602 (2012).
[47] B. A. Brown and W. D. M. Rae, Nucl. Data Sheets **120**, 115 (2014).
[48] L. Coraggio, A. Covello, A. Gargano, and N. Itaco, Phys. Rev. C **89**, 024319 (2014).
[49] S. Bogner, T. T. S. Kuo, and L. Coraggio, Nucl. Phys. A **684**, 432 (2001).
[50] S. Bogner, T. T. S. Kuo, L. Coraggio, A. Covello, and N. Itaco, Phys. Rev. C **65**, 051301(R) (2002).